Tellurium mineralization in the northern Organ district, Dona Ana County, New Mexico

Virgil W. Lueth
1998, pp. 265-269. https://doi.org/10.56577/FFC-49.265

in:

Las Cruces Country II, Mack, G. H.; Austin, G. S.; Barker, J. M.; [eds.], New Mexico Geological Society 49th Annual Fall Field Conference Guidebook, 325 p. https://doi.org/10.56577/FFC-49

This page is intentionally left blank to maintain order of facing pages.

TELLURIUM MINERALIZATION IN THE NORTHERN ORGAN DISTRICT, DOÑA ANA COUNTY, NEW MEXICO

VIRGIL W. LUETH
New Mexico Bureau of Mines and Mineral Resources, 801 Leroy Place, Socorro, NM 87801

Abstract—Telluride minerals in the northern Organ district occur in association with two distinct types of mineralization: (1) base metal sulfide mantos and (2) quartz vein and breccia bodies with gold, fluorite, sulfides, and tellurides. An east–west-trending fault served as the flowpath for mineralization with manto deposits localized by small anticlinal flexures in host Paleozoic sedimentary rocks. All manto deposits are confined to the dolomite units directly beneath the Percha Shale, a unit that acted as an impermeable barrier to ore fluids. Quartz vein and breccia deposits are present in the main fault, beneath the mantos, and in subsidiary cross-faults. Temperatures of mineralization, determined by homogenization temperatures of fluid inclusions (Th), overlap although mean temperatures in mantos (Th = 206°C) are higher than in the quartz-tellurium ores (Th = 178°C). Upper portions of the manto deposits are devoid of tellurides, while samples in close proximity to the quartz-tellurium ores contain the base metal tellurides, altaite (PbTe), and rickardite (Cu_7Te_5). The quartz-tellurium ores display a distinct paragenesis of galena-altaite-native tellurium, indicating increasing Te fugacity over time. Base metal telluride assemblages formed by reaction between preexisting sulfides and a tellurium-rich fluid.

INTRODUCTION

The Organ district in Doña Ana County, New Mexico, contains a wide variety of mineral deposits associated with the emplacement of the Organ batholith. Reports on the geology of the ore deposits in the district include: Lindgren et al. (1910), Dunham (1935), Albritton and Nelson (1943), Seager (1981), Newcomer and Giordano (1986), and McLemore et al. (1995). Tellurium mineralization, although reported by Dunham (1935), remained obscure until detailed mineralogical studies were done by Lueth (1988; 1989) and Lueth et al. (1988). Lueth and McLemore (this guidebook) reinterpreted metal zoning in the district utilizing metal ratios and mineral distributions. This paper provides a detailed summary of the mineralogy and presents information on the geochemistry of tellurium mineralization in the district.

GEOLOGY

The study area is located in the northern portion of the Organ mining district in the southern San Andres Mountains (Fig. 1). The San Andres Mountains, like the Organ mountains to the south, are a tilted fault-block mountain range characteristic of the Rio Grande rift tectonic province. Paleozoic marine sedimentary rocks lie unconformably on a Proterozoic basement of igneous and metamorphic rocks deformed by folding and faulting during a Laramide-age compressional event (Seager, 1981). After Laramide deformation, the area was intruded by the Organ batholith, part of a large batholith/caldera complex formed during the Oligocene. Silicic volcanic rocks associated with caldera development are not exposed in the study area but are found immediately to the north and south. Diverse types of ore mineralization appear to be associated with late-stage phases of the batholith (Seager, 1981; Lueth and McLemore, this guidebook). Later uplift and tilting of the ranges accompanied the development of the Rio Grande rift and resulted in the current attitude of the rock units in the Organ and San Andres Mountains.

The stratigraphy in the vicinity of the mines is dominated by carbonate rocks (Fig. 2), with dolomites predominating below the Devonian Percha Shale, and limestones more common in upper Paleozoic units. The Percha Shale strongly influences the distribution of certain ore deposits with carbonate replacement deposits occurring as mantos localized on the footwall side of the shale unit. Granitic dikes cut the sedimentary rocks but are relatively uncommon.

Ore deposits in the study area are localized along an east–west, high-angle fault on the northern margin of the Organ batholith (Fig. 2). This fault forms the basis of the Merrimac-Hilltop mineralization trend defined by Lueth and McLemore (this guidebook) and traverses sedimentary rocks ranging from Ordovician to Pennsylvanian. This structure has been mapped as a normal fault by both Dunham (1935) and Seager (1981); however the near-vertical nature of the fault surface makes classifying this fault ambiguous. This fault crosscuts intrusive rocks of the batholith and a 0.5 m

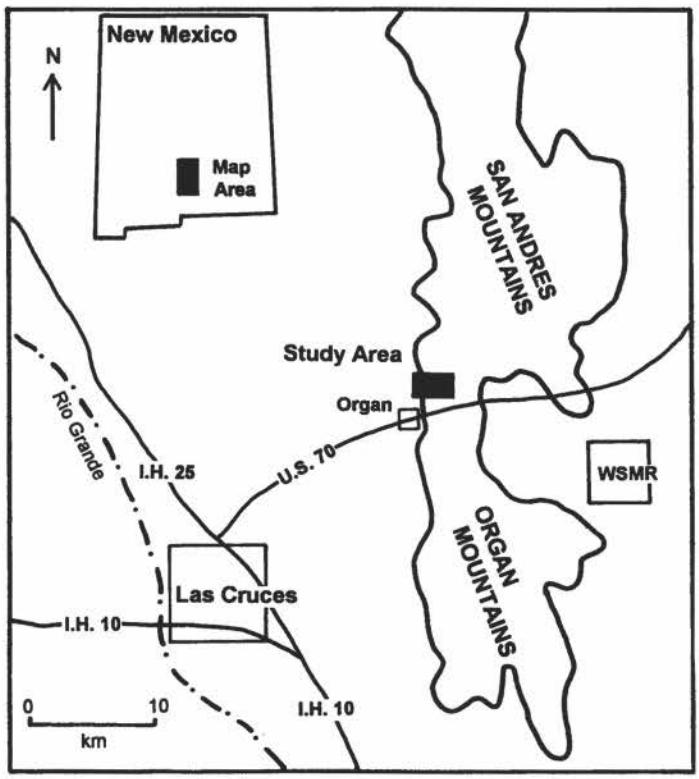

FIGURE 1. Location map of the study area, which is represented by the darkened rectangle.

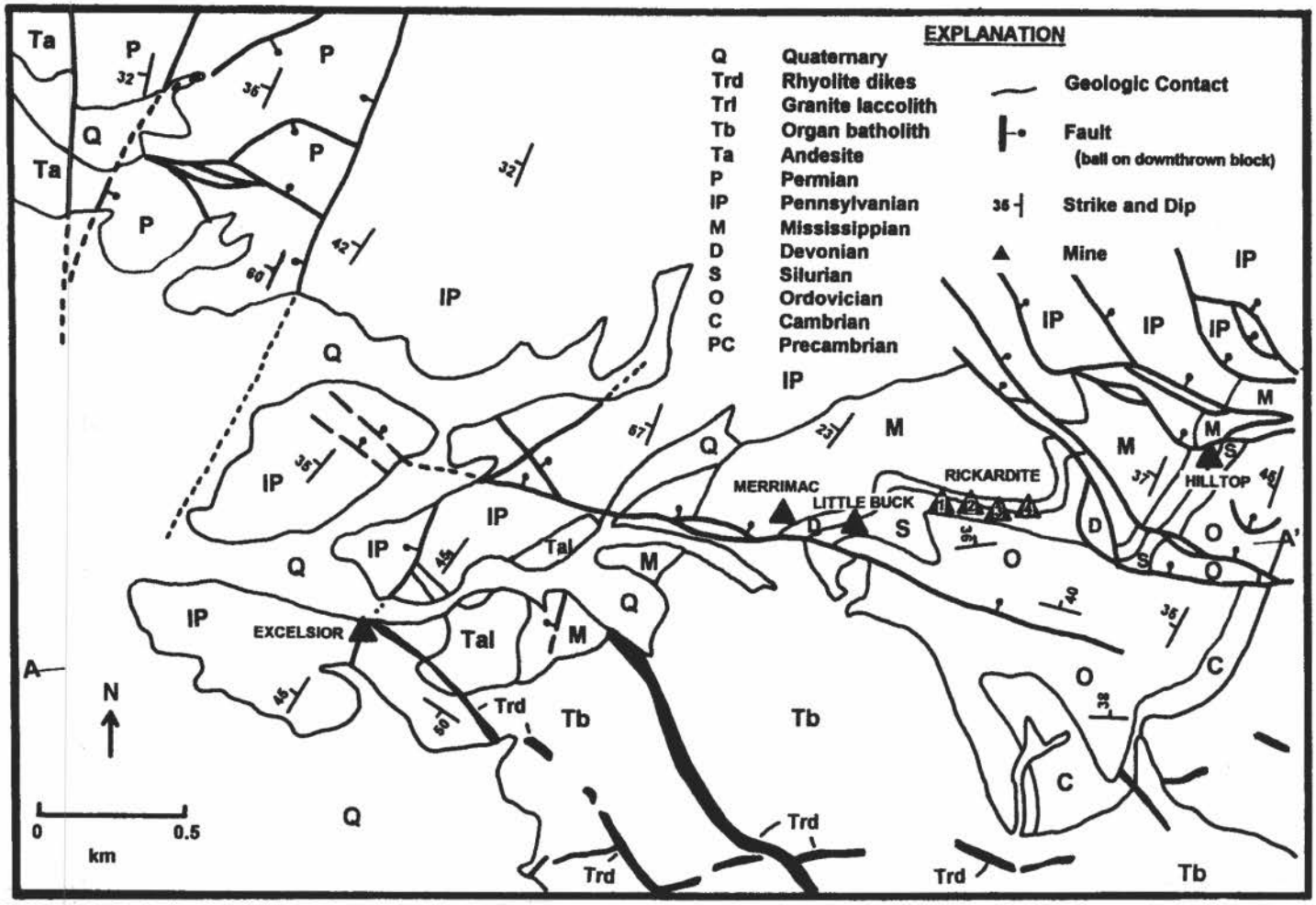

FIGURE 2. Geologic map of the northern Organ district. Map modified from Seager (1981). A-to-A' delineates the line of a cross section in Figure 4.

envelope of chlorite alteration is present, indicating post-intrusion movement and mineralization. Minor brecciation and drag-fold structures occur on both sides of the fault and banded quartz containing sparse sulfide mineralization fills the fault plane along its exposed length. Brecciation accompanies the quartz mineralization. Near the crests of small anticlinal folds, brecciation becomes more intense and expands upward in the fault zone (Fig. 3). Albritton and Nelson (1943) reported deposits localized on the crests of anticlines and similarly mineralized breccia bodies occur under the manto deposits at the Rickardite #2, #3, #4, and Hilltop deposits.

MINERALIZATION

Mineralization along the east–west-trending fault is distinctly zoned, based on mineral distributions and metal ratios (Lueth, 1988; Lueth and McLemore, this guidebook). Copper-zinc mineralization is dominant in the west and changes laterally to lead-silver ores to the east (Fig. 4). In the vicinity of the Merrimac mine, zinc-bearing skarns are the dominant type of deposit; eastward, zinc-lead replacement deposits are present at the Little Buck and Rickardite #1 and #2 mines. Zinc quantity diminishes, with lead comprising the dominant metal in lead-zinc replacements at the Rickardite #3, #4, and Hilltop deposits. Mineral distributions and metal zoning along this trend indicate that the origin of ore fluids was from near the Organ porphyry deposit (bordered by the Excelsior copper-bearing skarn) with solutions migrating east along the fault zone (Lueth, 1988; Lueth and McLemore, this guidebook).

Zinc skarn mineralization at the Merrimac mine, hosted by Mississipian limestones, consists of an ore assemblage dominated by sphalerite and chalcopyrite in a garnet-pyroxene gangue. Extensive destruction of skarn minerals, observed as calcsilicate alteration to actinolite and clay, is associated with sulfide mineralization, although sulfide minerals locally replace garnet and pyroxene with little alteration. Quartz and calcite are also associated with sulfide-stage deposition. Galena is present in small amounts associated with late-stage quartz veining. No telluride mineralization was noted in the zinc ores of the Merrimac mine. This is in contrast to a similar deposit at the Memphis mine, and in endoskarn deposits at the Quickstrike mine (Lueth et al., 1989), south of the study area where tetradymite (Bi_2Te_2S) is found in geochemically significant amounts.

Zinc-lead replacement deposits are present at the Rickardite #1, #2, and Little Buck mines, occurring at the contact between the Percha Shale and underlying Fusselman Dolomite. Dunham (1935) noted the presence of a solution breccia in the dolomite, and similar features are present also across the canyon along the east–west reverse fault discussed above (Fig. 3). Mineralization is localized on the crests of minor anticlinal folds, as noted by Albritton and Nelson (1943). Pyrite, sphalerite, galena, bornite, and chalcopyrite form manto and pipe deposits in dolomite. Very little alteration is present in the host dolomites other than the development of coarse-grained marble. Rarely, minor amounts of serpentine and talc are present at the contact between ore and marble, probably as a consequence of solution reaction with the dolomite. Bornite is the principal copper mineral at the Rickardite No. 1 and 2 mines and chalcopyrite occurs in minor amounts as exsolution features in sphalerite. Tennanite is present in some of

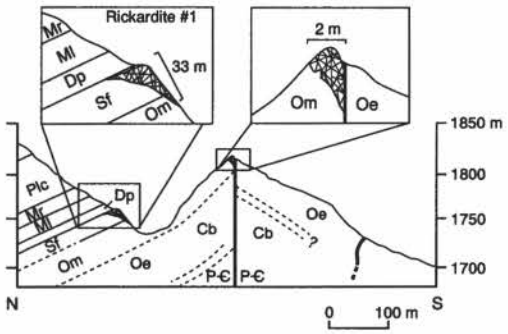

FIGURE 3. Geologic cross section of the Rickardite #1 mine area, view toward the east. Breccia mineralization, identical to the breccia body beneath the orebody, is present across the canyon from the mine. Vertical exaggeration is 1.75x. Diagram adapted from Lueth (1988).

the manto ores at the Little Buck (Lueth et al., 1989). Gold is reported at the Little Buck mine, associated with quartz (Dunham, 1935). Dunham also reported high silver and tellurium assays in the ores and suggested hessite was present. Hessite (Ag_2Te) was confirmed by Lueth et al. (1989), observed as inclusions in galena associated with the quartz ores. Rickardite (Cu_3Te_7) and altaite (PbTe) are reported at the Ricardite #3, and #4 mines (Lueth et al., 1989). No gold tellurides were observed.

Lead-zinc replacement deposits are present at the Rickardite #3, #4, and Hilltop mines in similar geologic relationships to the zinc-lead deposits. Galena is the dominant sulfide mineral with lesser amounts of pyrite, sphalerite, and rare chalcopyrite in an interlocking mosaic texture. The deposits tend to be lenticular, although the upper ore body at the Hilltop mine is more tabular than those of the Rickardite and Little Buck deposits. A gold-bearing quartz orebody is located beneath the base-metal manto at the Hilltop mine in a similar relationship to the quartz-breccias beneath the Rickardite and Little Buck deposits. Small, millimeter-scale veins of galena, altaite, fluorite, and native tellurium also crosscut the manto and quartz ores. Electron microprobe analysis of the ores reveals that altaite, native tellurium, and hessite are present as inclusions in the vein galena (Lueth, et al., 1989). Rickardite was identified at the Ricardite #3 mine (Lueth et al., 1989) replacing chalcopyrite exsolution lamellae in sphalerite.

A generalized paragenesis can be determined for the two types of orebodies observed in the study area (Fig. 5). Within the manto deposits the sequence of mineralization begins with pyrite and progresses through bornite, chalcopyrite, sphalerite, and argentiferous galena (galena with inclusions of acanthite). This paragenesis mimics the ore zoning along the east–west Merrimac-Hilltop trend. Paragenetic relationships in the quartz-tellurium ores were based on the occurrences at the Hilltop and Rickardite deposits. Gold was deposited very early and was never noted in contact with other tellurides or sulfides, and was observed exclusively at the contact between quartz and dolomitic marble. Hessite is only observed as inclusions precipitated with galena, such as at the Little Buck and Hilltop mines. Altaite and native tellurium are present in discrete grains and as inclusions in galena, as well as in late-stage, northwest-trending veinlets of altaite and native tellurium.

Fluid inclusion microthermometry on inclusions in quartz, fluorite, and sphalerite was used to determine mineralization temperatures in the manto and quartz-telluride ores. All samples were analyzed on a gas-flow stage at the University of Texas at El Paso with two main types of inclusions identified. The most common was a two-phase type with liquid volumes greater than vapor. The second type are carbon dioxide-bearing inclusions, only observed in the quartz-telluride ores. Results of the microthermometry study are presented in Figure 6. Two overlapping but statistically distinct populations of temperatures are recognized (Lueth et al., 1989). Manto ores tend to cluster about a mean homogenization temperature of 206°C and the quartz ores have a mean homogenization temperature of 178°C. Higher temperature "outliers" in the quartz ores extend to temperatures greater than 300°C. Salinities in both groups range between 0 and 6 eq. wt.% NaCl equivalent. Fluid inclusion temperatures from fluorite in the quartz-tellurium ores at the Hilltop mine have a mean value of 175°C with very little variation in homogenization temperatures. (Lueth, 1988). In addition, carbon dioxide is present in some of the fluorite and quartz samples from the Hilltop mine. Fluid inclusion

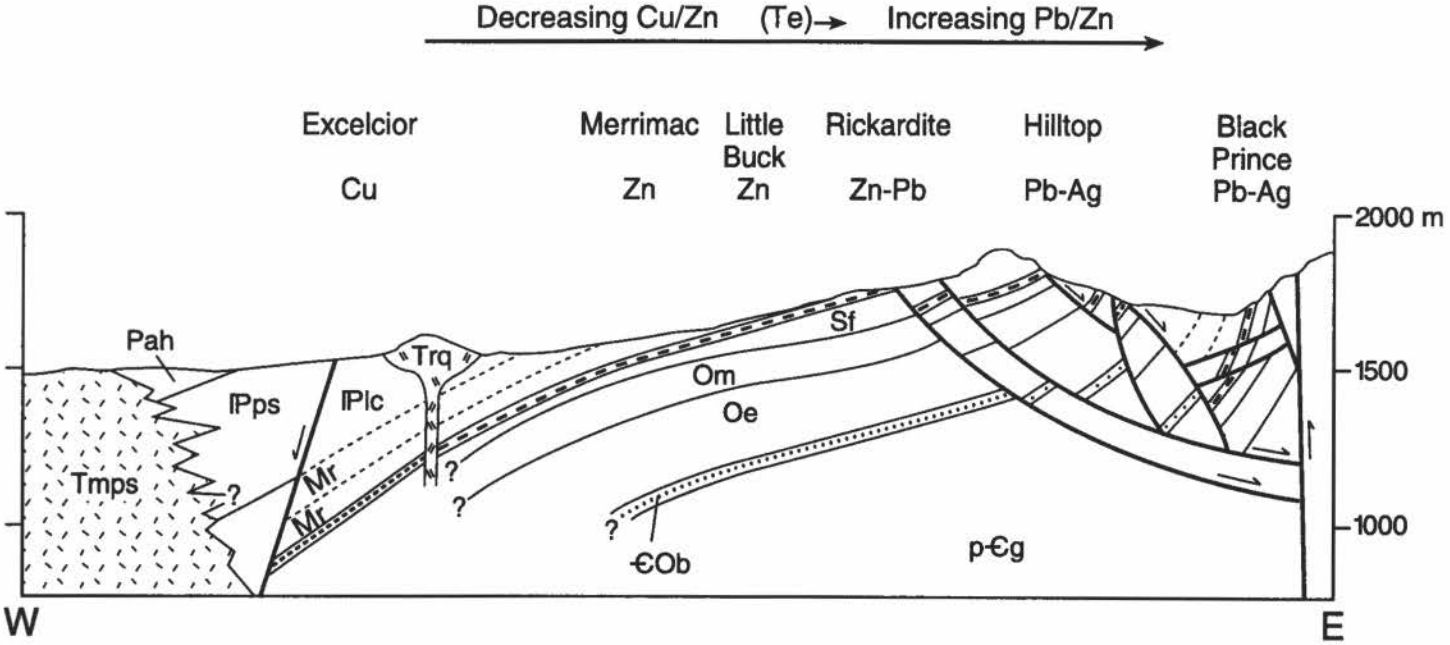

FIGURE 4. Geologic cross section of the study area along the Excelsior-Black Prince mineralization trend defined by Lueth (1988). Ore type and relative zoning are indicated. Telluride occurrences occur east of the Little Buck mine as noted by (Te). Horizontal distance of the cross-section is 4 km. Diagram adapted from Lueth (1988).

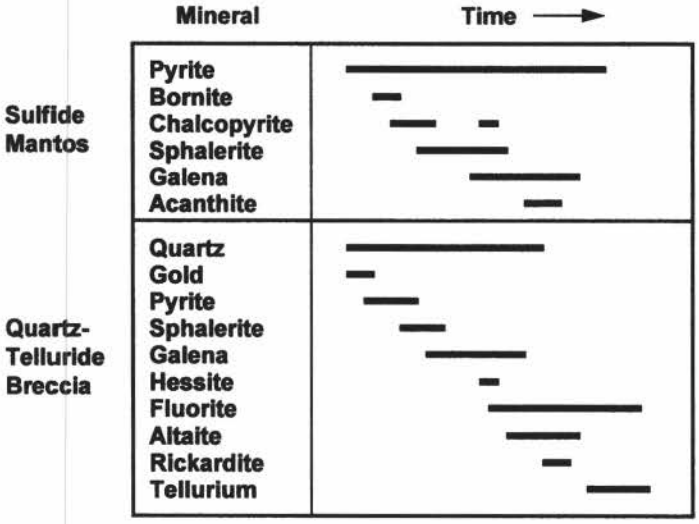

FIGURE 5. Paragenesis diagram for the ore types in the study area.

homogenization temperatures in quartz ores from the Little Buck mine average 180°C in both sphalerite and coexisting quartz.

DISCUSSION

Geologic, mineralogic, and geothermometric data indicate that northern Organ district manto ores are paragenetically distinct from spatially related quartz-telluride ores. The mantos contain early assemblages consisting of galena-sphalerite-pyrite-bornite/chalcopyrite. This assemblage is typical of carbonate replacement deposits and, among the deposits studied, varies only in relative mineral proportions. Mineral distributions are reflected in a zoning pattern established along the mineralization trend. Lueth (1988) and Lueth and McLemore (this guidebook) inferred that zoning reflected the relative solubilities of the metal complexes responsible for metal transport. Tellurides occur only sporadically in the sulfide ores and are most common at the contact with later, structurally-hosted, cross-cutting quartz-telluride mineralization, especially at Little Buck and Hilltop mines.

Gold deposition is the first stage associated with quartz-telluride

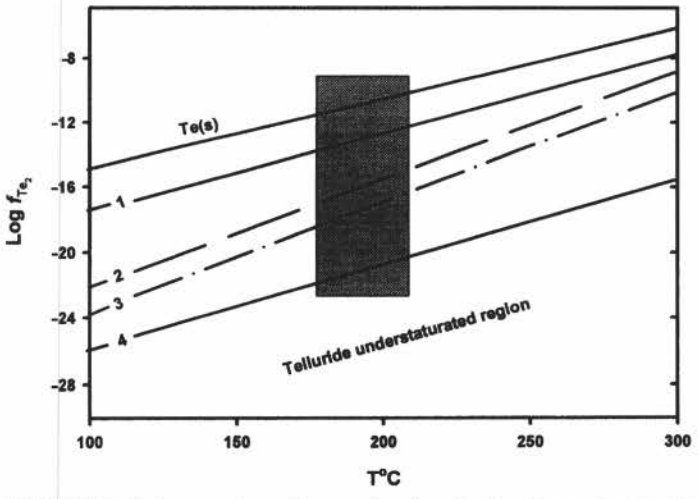

FIGURE 7. f_{Te2}-temperature diagram showing the locations of some telluride reactions at different f_{S2} buffers: (1) gold-calaverite, (2) galena-altaite at f_{S2} = pyrrhotite-pyrite, (3) argentite-hessite at f_{S2} = chalcopyrite-bornite-pyrite, and (4) silver-hessite. Diagram modified from Afifi et al. (1988a) utilizing data from Afifi et al. (1988b). The shaded area represents the range in temperature and f_{Te2} inferred from fluid inclusion data (Lueth, 1988) and mineral assemblages observed from ores in the study area.

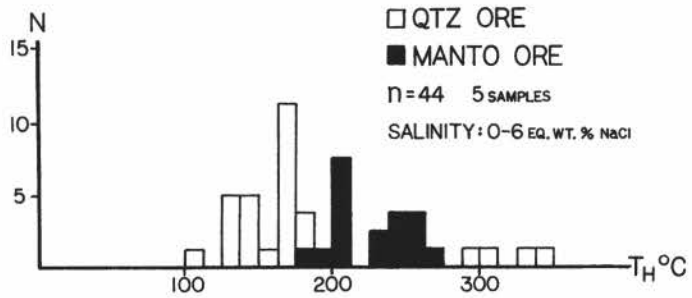

FIGURE 6. Histogram of fluid inclusion homogenization temperatures in the study area. Data from Lueth (1988).

mineralization at the Hilltop mine. In close proximity to gold, but not in contact, is galena with hessite inclusions. The presence of hessite as inclusions in galena indicate tellurium fugacities above the argentite-hessite reaction (Fig. 7, line 4) but below the galena-altaite (Fig. 4, line 2) and gold-calaverite (Fig. 7, line 1) reactions at the temperature range derived from fluid inclusion analyses. Altaite-hessite-galena succeeds the gold-altaite assemblage and indicates increasing tellurium fugacity with time. The latest paragenetic assemblage, observed in crosscutting veins, consists of altaite-native tellurium. Early precipitation of gold and isolation from later tellurium-rich fluids, by precipitation of insulating quartz(?), accounts for the lack of gold telluride minerals. The abundance of altaite in the deposit is due to extensive buffering of the high Te fugacity solutions by the Pb-bearing manto ores following the reaction of Afifi et al. (1988a): $2PbS + Te_2 = 2PbTe + S_2$.

Where native tellurium is observed in veinlets with altaite, it is not in contact with the manto ores. In the absence of reactive sulfides, Te activity increased to the point where native Te became stable in the veinlets. Native tellurium inclusions in galena represent residual metastable phases that did not react to completion or represent exsolution features.

Fluid inclusion data supports two separate periods of mineralization, although overlap of the data may suggest that evolution of a single fluid over time gave rise to the distinct stages of ore deposition. Fluid inclusions in quartz from manto ores display higher average homogenization temperatures (Th) compared to the quartz-telluride ores. Manto ores average Th = 220°C, with low

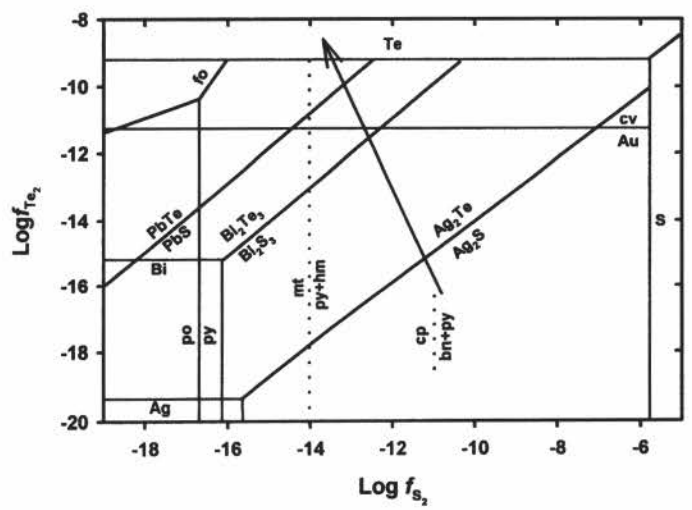

FIGURE 8. Relative variations in Te_2 and S_2 fugacities with respect to selected telluride-sulfide-oxide equilibria at 200°C. The arrow represents the general trend observed in the ores from the study area. Phase equilibria calculated from data presented by Afifi et al. (1988b). Abbreviations: bn = bornite, cp = chalcopyrite, cv = calaverite, fo = frohbergite, hm = hematite, mt = magnetite, po = pyrrhotite, py = pyrite.

salinities, similar to other carbonate replacement deposits (McLemore and Lueth, 1996). Quartz-telluride mineralization averages Th = 187°C with salinities less than 6 wt.% NaCl equivalent, typical of telluride systems described by Afifi et al. (1988a). The presence of fluorite is unique to the quartz-telluride ores, and carbon dioxide-bearing fluid inclusions in the quartz-telluride ores are also distinctive. The occurrence of fluorite in the ores and CO_2 in inclusions suggests the telluride-bearing fluid was acidic and CO_2 was liberated when the fluids reacted with the enclosing carbonate rocks. Tellurium may have been complexed as the hexafluoride that provided the components for the formation of associated fluorite.

The mineral assemblages and paragenesis of both the sulfide mantos and quartz-telluride breccias reflect the evolution of the mineralizing solutions. Within the mantos, evidence of decreasing sulfur activity is apparent in the copper sulfide mineralogies (Fig. 7). Bornite at the Rickardite #1 and #2 mines is replaced by chalcopyrite, the dominant copper phase in the lead-bearing mantos at the Rickardite #3, #4, and Hilltop deposits. Sulfur activity would be expected to decrease with time due to the precipitation of sulfide minerals with no additional sulfur input. Relative to sulfur, tellurium activities would increase with time. This is a common feature in tellurium deposits with the assemblage galena-altaite-native tellurium noted at other deposits where tellurium activities increase over time (Afifi, 1988a). At the Hilltop mine, increasing tellurium activity is observed as replacement of galena by altaite and later native tellurium. Figure 8 illustrates a hypothetical evolutionary pathway for fluids illustrating the increase of tellurium fugacity over time as represented by the ores. Initial precipitation of sulfides is followed by precipitation of hessite and galena with gold. Gold precipitated early in the paragenesis prior to the saturation of gold telluride. Galena-hessite is replaced by altaite-galena and eventually gives way to altaite-tellurium assemblages late in the paragenesis of the Hilltop deposit. The occurrence of rickardite replacing chalcopyrite at the Rickardite mine suggests a Te-rich fluid reacted with a pre-existing sulfide, analogous to the formation of altaite. The lack of pyrrhotite in the sulfide ores and frohbergite ($FeTe_2$) in the telluride deposits limits sulfur fugacities below the pyrite-pyrrhotite buffer. No magnetite was observed in the ores further limiting the sulfur fugacity below the magnetite-pyrite+hematite buffer.

The origin of the Te-rich fluid responsible for telluride mineralization is speculative. However, other workers attribute telluride mineralization to late-stage fractionation products of crystallizing intermediate to granitic intrusions (Afifi et al., 1988b). A late-stage granite laccolith is present in the vicinity of the mines (Fig. 2, map unit: Tal). This intrusion contains numerous hydrothermal alteration features, including silicification, emanating from the laccolith that can be traced via mapping into the east–west, ore-related fault zone (Lueth, 1992). Chemical analyses of the laccolith show it is enriched (with respect to average crustal abundance in granite as presented by Levinson, 1980) in gold (2x), molybdenum (17x), copper (19x), lead (40x), and zinc (4x). None of the deposits west of the laccolith or those that are unrelated via known faults or fractures to the fault zone, contain tellurides. Work continues on the origin of the fluids in the vicinity of this laccolith.

CONCLUSIONS

The sulfide-manto and quartz-telluride orebodies in the northern portion of the Organ district represent two distinct episodes of mineralization that utilized similar structures. Telluride ores cross cut manto deposits and tellurides replace sulfides establishing the relative timing between the two types of deposits. Although telluride mineralization postdates sulfide ores, both deposits could be related to the same hydrothermal source. The presence of tellurium mineralization possibly associated with late-stage magmatism represents a new exploration target for precious metal telluride deposits in the district.

ACKNOWLEDGMENTS

This work was supported by the New Mexico Bureau of Mines and Mineral Resources (Charles E. Chapin, Director and State Geologist). Partial funding for this project was provided by the Organized Research Grant program at Tarleton State University, Stephenville, Texas. Fluid inclusion and electron microprobe analyses were performed at the University of Texas at El Paso. Nicholas E. Pingitore (UTEP) assisted with the microprobe analyses. Ramon Llavona helped with field collection, sample preparation, and fluid inclusion analysis. Phillip Goodell (UTEP), William X. Chavez (NMIMT), and Bruce Geller (Geoconcepts, Littleton, CO) served as reviewers and provided constructive suggestions for the improvement of the manuscript. Sam Seek arranged access to WSMR and range riders, Rod Pino and Chris Ortega, provided transportation on the range.

REFERENCES

Afifi, A. M., Kelley, W. C. and Essene, E. J., 1988a, Phase relations among tellurides, sulfides, and oxides II; Applications to telluride-bearing ore deposits: Economic Geology, v. 83, p. 395–404.

Afifi, A. M., Kelley, W. C. and Essene, E. J., 1988b, Phase relations among tellurides, sulfides, and oxides I; Thermochemical data and calculated equilibria: Economic Geology, v. 83, p. 377–395.

Albritton, C. C. and Nelson, V. E., 1943, Lead, zinc, and copper deposits of the Organ district, New Mexico (with a supplement on the occurrence of bismuth): U.S. Geological Survey, Open-file Report 43, 39 p.

Dunham, K. C., 1935, The geology of the Organ Mountains: New Mexico Bureau of Mines and Mineral Resources, Bulletin 11, 270 p.

Levinson, A. A., 1980, Introduction to exploration geochemistry: Applied Publishing, Wilmette, Illinois, 924 p.

Lindgren W., Graton, L. C. and Gordon, C. H., 1910, The ore deposits of New Mexico: U.S. Geological Survey, Professional Paper 68, 361 p.

Lueth, V. W., 1988, Studies of the geochemistry of the semimetal elements: Arsenic, antimony, and bismuth [Ph.D. dissertation]: El Paso, University of Texas, 173 p.

Lueth, V. W., 1989, Characterization of tellurium mineralization in the Organ district, New Mexico: Geological Society of America, Abstracts and Programs, v. 21, no. 6, p. A149.

Lueth, V. W., 1992, Origin of reversed textural featues in a granite laccolith, Organ district, New Mexico: Geological Society of America, Abstracts and Programs, v. 24, no. 6, p. A 49.

Lueth, V. W., Goodell, P. C., Llavona, R., Mertig, H. and Sharp, W., 1988, Tellurium minerals of the Organ district, Doña Ana County, New Mexico (abstr.): New Mexico Geology, v. 10, p. 18.

McLemore, V. T. and Lueth, V. W., 1996, Lead-zinc deposits in carbonate rocks in New Mexico: Society of Economic Geologists, Special Publication 4, p. 264–270.

Newcomer, R. W. and Giordano, T. H., 1986, Porphyry-type mineralization and alteration in the Organ mining district, south-central New Mexico: New Mexico Geology, v. 8, p. 83–86.

Seager, W. R., 1981, Geology of the Organ Mountains and southern San Andres Mountains, New Mexico: New Mexico Bureau of Mines and Mineral Resources, Memoir 36, 97 p.

Well-developed columnar jointing in a late Oligocene basalt flow exposed in "The Narrows", about 2 mi west of Hillsboro. Photograph by Greg Mack.